

# Optimizing the Desorption Technology of Total Flavonoids of *Ginkgo Biloba* from Separating Materials of Activated Carbon

Lihu Zhang, Xiaomeng Zhang, Qi Li, Wei Xiao,\* Erzheng Su, Fuliang Cao, and Linguo Zhao\*

Cite This: *ACS Omega* 2021, 6, 35002–35013

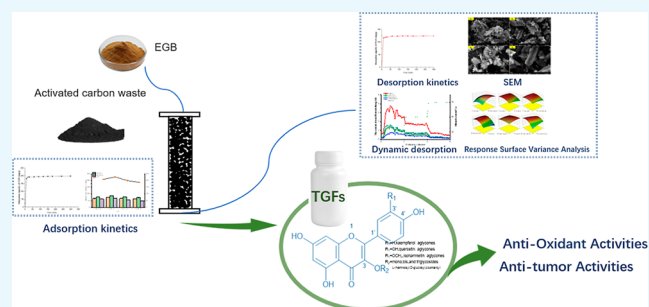
Read Online

ACCESS |

Metrics &amp; More

Article Recommendations

**ABSTRACT:** Activated carbon adsorption is one of the processes used to produce ginkgolides from the extract of *Ginkgo biloba* (EGB) in most enterprises. However, the problem is that the ginkgolides can be eluted by ethanol after the *Ginkgo biloba* extracts are adsorbed by activated carbon, while total ginkgo flavonoids (TGFs) would form dead adsorption, leading to the ineffective utilization of TGFs. In this paper, the maximum adsorption capacity of TGFs by activated carbon was 226.7 mg/g activated carbon at pH 5, and the adsorption of TGFs was easier and more favorable to monolayer adsorption. On this basis, the technical process of desorption of TGFs from activated carbon preparation technology was optimized by using the response surface optimization technique. Under the optimum process (the elution volume was 116.75 mL, the ethanol concentration in the eluent was 73.4%, the elution temperature was 31.5 °C, and the ammonia concentration was 5.7%), the desorption rate of TGFs was 74.56%. Scanning electron microscopy morphological analysis showed that the used activated carbon had a wide pore size distribution, with the micropore pore size mainly concentrated around 0.64 and 1.00 nm and the mesopore pore size mainly concentrated between 2.89 and 39.5 nm. In addition, the molecular weight of ginkgo flavonoids is mainly distributed between 500 and 1000 Da, which can be transported to the micropores through the mesopore channels. On the other hand, there is a force between the flavonoids and the acidic oxygen-containing functional groups on the pore surface, which is the main reason for the formation of dead adsorption. The obtained results contribute to further improving the process of adsorbing and desorbing TGFs from EGB and lay a foundation for the development of more suitable activated carbon.



Under the optimum process (the elution volume was 116.75 mL, the ethanol concentration in the eluent was 73.4%, the elution temperature was 31.5 °C, and the ammonia concentration was 5.7%), the desorption rate of TGFs was 74.56%. Scanning electron microscopy morphological analysis showed that the used activated carbon had a wide pore size distribution, with the micropore pore size mainly concentrated around 0.64 and 1.00 nm and the mesopore pore size mainly concentrated between 2.89 and 39.5 nm. In addition, the molecular weight of ginkgo flavonoids is mainly distributed between 500 and 1000 Da, which can be transported to the micropores through the mesopore channels. On the other hand, there is a force between the flavonoids and the acidic oxygen-containing functional groups on the pore surface, which is the main reason for the formation of dead adsorption. The obtained results contribute to further improving the process of adsorbing and desorbing TGFs from EGB and lay a foundation for the development of more suitable activated carbon.

## 1. INTRODUCTION

*Ginkgo biloba* is the only remaining large plant in the *Ginkgo* family. In the 1960s, German and French scientists were the first to extract components (*Ginkgo biloba* flavonoids and ginkgolide) from *Ginkgo biloba* leaves to treat cardiovascular diseases. The extract of *Ginkgo biloba* (EGB), the main contents of which are ginkgo flavonoids and ginkgolide, has significant biological activity and important application value. Most of the existing *Ginkgo biloba* pharmaceuticals are developed with EGB that meets the Chinese Pharmacopoeia standard as the main raw material, while total *Ginkgo biloba* flavonoids (TGFs) and ginkgolides have obvious differences in biological activity. Ginkgolides are one of the most commonly used natural medicines for treating the central nervous system and cardiovascular diseases,<sup>1–5</sup> which have been approved by the China National Drug Administration to enter clinical research. Therefore, the preparation technology of ginkgolides with high yield and low cost has played a key role in the development and utilization of related products.

So far, activated carbon adsorption is one of the processes employed for producing ginkgolides from EGB in related enterprises. The main problem is that after the activated carbon adsorbs EGB from ginkgolide leaves, ginkgolides can be eluted

by ethanol, while TGFs form dead adsorption, leading to ineffective utilization of TGFs, and increase the use of activated carbon.<sup>6</sup> In addition, there is no report to solve the problem of dead adsorption after adsorption of TGFs by activated carbon and the method of “one-step” simultaneous preparation of TGFs and ginkgolides.

TGFs are a natural, free radical scavenger and vasodilator, which can significantly reduce the damage to cardiac and brain tissue cells caused by excessive free radicals during ischemia and hypoxia and aging and can promote the improvement of blood rheology. Besides, TGFs contain a large number of reducing hydroxyl functional groups, which can prevent and inhibit the toxicity of oxygen-free radicals, reducing the peroxidation damage of lipid and other pathological damage to the human body. It can play the role of antioxidant, scavenge oxygen-free

Received: October 11, 2021

Accepted: November 30, 2021

Published: December 10, 2021



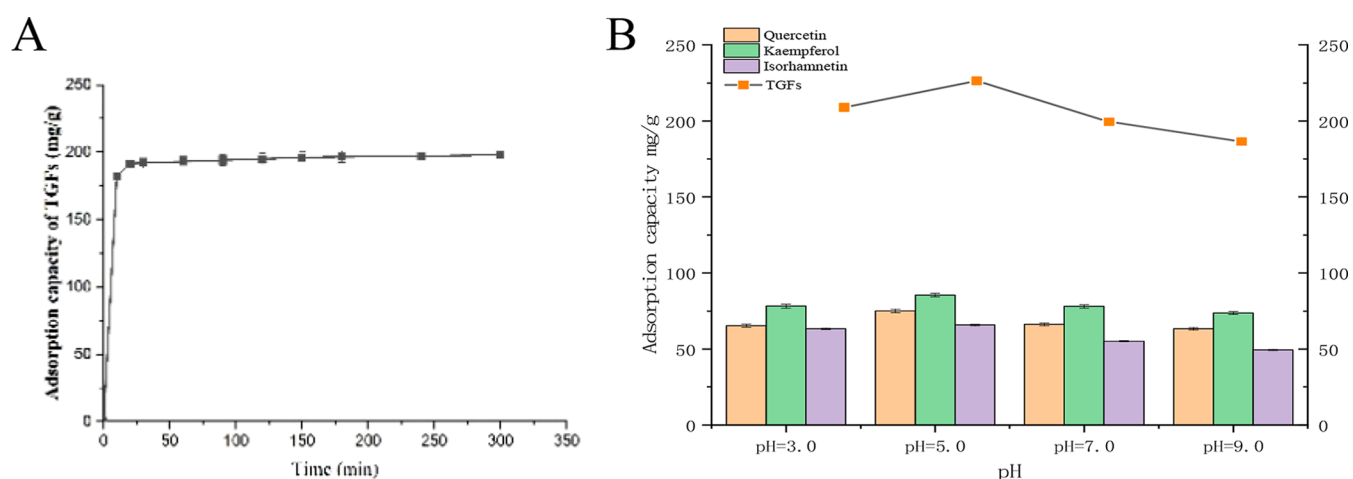


**Figure 1.** Static adsorption curve of TGFs in EGB (A) and effect of pH on static adsorption of TGFs by activated carbon (B). (A) 1.5 g of activated carbon with addition of 1.5 g of EGB (dissolved with 100 mL 10% ethanol) was oscillated at 30 °C for 180 r/min at 10–300 min. Sampling was 1 mL; the adsorption capacity and column loading of TGFs were determined. (B) pH value of the sample solution of EGB was adjusted to 3, 5, 7, and 9. 0.2 g of activated carbon was weighed, and EGB was dissolved in 100 mL of 10% ethanol. Adsorption equilibrium of TGFs on activated carbon was determined after 180 rpm oscillation for 6 h at 30 °C in a constant-temperature oscillator.

radicals, regulate the activity of superoxide dismutase and catalase, and scavenge NO-free radicals.<sup>7</sup> Therefore, if the problem of the formation of dead adsorption of TGFs on activated carbon is solved, the performance of adsorption and desorption of TGFs on activated carbon is investigated, and the process of desorption of TGFs on activated carbon is established, it is expected that the simultaneous preparation of ginkgolide and TGFs can be realized.

In this study, the static adsorption curves of activated carbon on TGFs were investigated, and the effects of various adsorption factors on the ability of activated carbon to adsorb TGFs were analyzed. Based on these obtained results, the influencing factors of the process of activated carbon for the resolution of TGFs were optimized using the response surface optimization method, and the performance indexes such as the pore structure and the pore size distribution of the used activated carbon were investigated. The results of the study are beneficial to further improve the process of adsorption and desorption of total ginkgo flavonoids (TGF) and lay the foundation for screening more suitable activated carbon, which can provide technical support for solving the technical bottleneck faced by enterprises in the simultaneous preparation of ginkgolides and TGFs.

## 2. RESULTS AND DISCUSSION

### 2.1. Study on Adsorption Conditions of Activated Carbon for TGFs.

#### 2.1.1. Kinetic Curve of Static Adsorption of TGFs on Activated Carbon.

The static adsorption method of activated carbon has its unique advantages. Due to the high selectivity of adsorbent materials and the low cost and high saturation capacity of the adsorbent, it not only solves the expensive problem of chemical methods but also overcomes the disadvantages of limited adsorption capacity of biological methods.<sup>8</sup>

The adsorption behavior of static adsorption of activated carbon can be understood by examining the relationship between the adsorption amount of TGFs adsorbed by activated carbon and time. The eluates of adsorption were collected at different time points, and the static adsorption curves of activated carbon on ginkgo flavonoids in EGB were obtained as shown in Figure 1A. According to the adsorption kinetics curve

of activated carbon, with the increase of time, the adsorption capacity of activated carbon on TGFs increased significantly. The whole process could be divided into three stages. The adsorption index of TGFs increased at the first stage (0–10 min), namely, the linear growth period, and the equilibrium state of adsorption approached in the range of 10–90 min, which can be considered as a slow growth period. After 90 min, the adsorption and desorption capacities stabilized at a fixed value, which was a stable period. To ensure the saturation of adsorption, the experimental period in the later stage was approximately 4 h. Finally, the maximum adsorption capacity of TGFs by activated carbon was 195.8 mg/g activated carbon.

#### 2.1.2. Effect of pH on Static Adsorption of TGFs by Activated Carbon.

Till now, more than 40 kinds of flavonoids have been isolated, including 25 kinds of monoflavones and glycosides, mainly composed of quercetin, kaempferol, isorhamnetin, and mono-, di-, and triglycosides.<sup>9–11</sup> The mechanism of the treatment of the TGFs by activated carbon adsorption or reduction varied according to the different pH values of the aqueous solution. The pH value of the sample solution of TGFs was adjusted to 3, 5, 7, and 9, respectively. The adsorption time was 4 h, and the adsorption temperature was 35 °C. The adsorption amount and the TGF content of the three main ingredients (quercetin, kaempferol, and isorhamnetin) were calculated. The results were obtained and are displayed in Figure 1B. The pH exhibited a great influence on the adsorption of TGFs by activated carbon. The largest adsorption capacity of TGFs occurred when the pH value was 5, and the maximum adsorption capacity of TGFs by activated carbon was 226.7 mg/g activated carbon. At the same time, the two components quercetin and kaempferol also reached a higher level when the pH value was 5. The reasons for this result are as follows: Because there are numerous hydroxyphenyl structures and glycoside bonds in the structure of flavonoids,<sup>12</sup> these compounds are weakly acidic; the adsorption effect is more favorable under weak acidic or acidic conditions, and the pH of the upper sample is more suitable to control around 5.

#### 2.1.3. Isothermal Constants of Activated Carbon Adsorption of TGFs.

The constant of isotherm is an important index describing the balance of binding force between activated carbon and adsorbed components.<sup>13</sup> Langmuir and Freundlich

Table 1. Langmuir and Freundlich Equation Parameters for Adsorption of TGFs by Activated Carbon

	T/°C	Langmuir equation	R <sup>2</sup>	Freundlich equation	R <sup>2</sup>
quercetin	25	$Q_e = (146.67C_e)/(8.04 + C_e)$	0.9974	$Q_e = 26.55C_e^{0.472}$	0.9974
	30	$Q_e = (132.14C_e)/(7.61 + C_e)$	0.9998	$Q_e = 31.73C_e^{0.358}$	0.9820
	35	$Q_e = (141.43C_e)/(6.52 + C_e)$	0.9991	$Q_e = 28.90C_e^{0.491}$	0.9861
kaempferol	25	$Q_e = (205.73C_e)/(8.43 + C_e)$	0.9946	$Q_e = 32.53C_e^{0.526}$	0.9946
	30	$Q_e = (170.32C_e)/(6.97 + C_e)$	0.9923	$Q_e = 39.33C_e^{0.386}$	0.9895
	35	$Q_e = (184.15C_e)/(6.05 + C_e)$	0.9899	$Q_e = 35.50C_e^{0.514}$	0.9651
isorhamnetin	25	$Q_e = (118.65C_e)/(9.78 + C_e)$	0.9916	$Q_e = 13.62C_e^{0.660}$	0.9946
	30	$Q_e = (77.90C_e)/(6.46 + C_e)$	0.9900	$Q_e = 16.34C_e^{0.449}$	0.9750
	35	$Q_e = (94.99C_e)/(6.00 + C_e)$	0.9750	$Q_e = 16.22C_e^{0.600}$	0.9563
TGFs	25	$Q_e = (462.73C_e)/(24.97 + C_e)$	0.9936	$Q_e = 39.10C_e^{0.545}$	0.9978
	30	$Q_e = (383.81C_e)/(21.39 + C_e)$	0.9903	$Q_e = 55.89C_e^{0.395}$	0.9871
	35	$Q_e = (433.71C_e)/(18.98 + C_e)$	0.9637	$Q_e = 43.66C_e^{0.536}$	0.9280

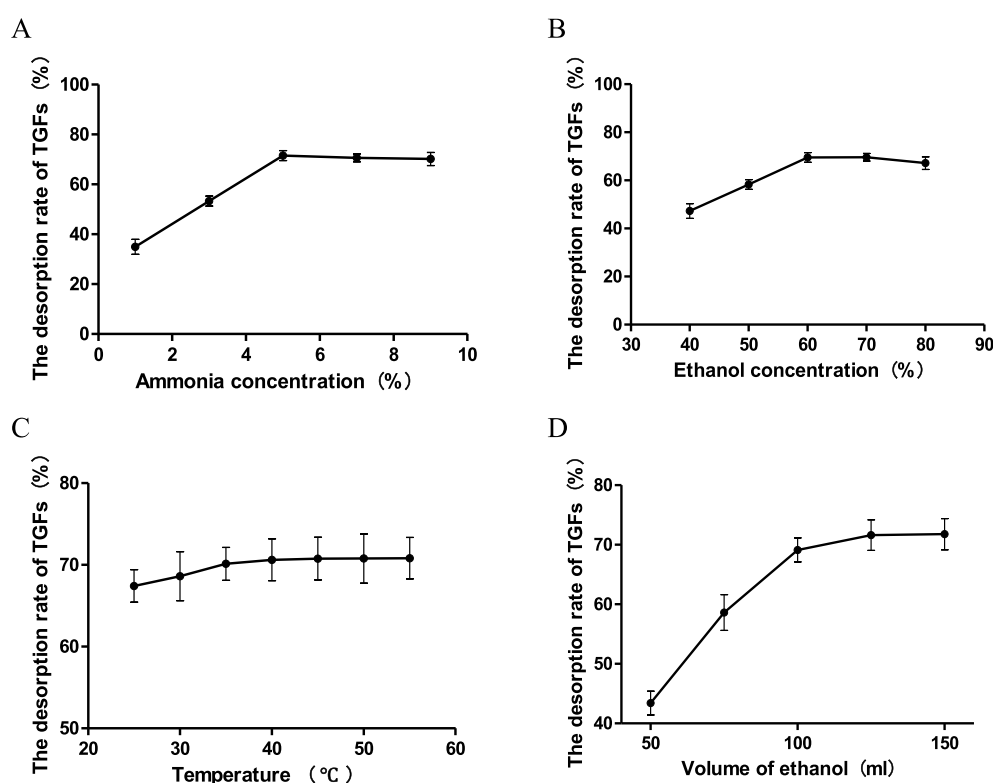


**Figure 2.** Influence of ammonia concentration (A), ethanol concentration (B), temperature (C), and ethanol volume (D) on the elution rate. (A) Effects of the ammonia concentration on the extraction rate were 1, 3, 5, 7, and 9%. (B) Effects of the ethanol concentration on the extraction rate were 40, 50, 60, 70, and 80%. (C) Effects of the extraction temperature on the extraction rate were as follows 25, 30, 35, 40, 45, 50, and 55 °C. (D) Effects of the ethanol volume on the extraction rate were 50, 75, 100, 125, and 150 mL. In each group, 0.75 g of EGB was dissolved in ethanol solution and adsorbed by 1.5 g of activated carbon for the elution experiment.

are two commonly used isotherm adsorption equations. Generally speaking, the Langmuir isotherm equation is suitable for the surface adsorption of the monolayer. Because there is no interaction between adsorbed molecules, the adsorption force is single. The Freundlich equation can be used for the equilibrium condition of multilayer adsorption. Langmuir and Freundlich's equations were fitted to the data of total flavonoids and three flavonoid aglycones of *Ginkgo biloba* at different temperatures. The specific constants are shown in Table 1.

The equilibrium adsorption capacity was ordinate, and the equilibrium concentration was abscissa. The adsorption isotherms under different conditions were obtained. The experimental results were fitted by the Langmuir equation (eq 2) and the Freundlich equation (eq 3), where  $Q_e$  is the

maximum adsorption capacity (mg/g) and  $C_e$  is the concentration at equilibrium (mg/mL).

As shown in Table 1, the constant  $K_L$  in the Langmuir equation indicates the binding capacity between the adsorbent and the adsorbed molecule, and  $Q_m$  indicates the maximum adsorption capacity of the adsorbent on the adsorbed molecule; the larger the  $K_L$  and  $Q_m$ , the easier the TGFs in *Ginkgo biloba* extract are adsorbed by the activated carbon. In addition, adsorption is an exothermic reaction and low temperature is favorable for adsorption, but too low a temperature increases the viscosity of the solution of *Ginkgo biloba* and other substances and is not conducive to be adsorbed. The Freundlich equation for TGF adsorption constant  $1/n$  values ranged from 0.1 to 0.55. When the  $1/n$  value is greater than 1, it means that the adsorbent finds it hard to adsorb the small molecules, which indicated that

TGF adsorption was easier by activated carbon. The  $1/n$  value in the Freundlich equation is located between 0.1 and 0.5, which shows that the adsorbent is easy to adsorb. In addition, the Langmuir of activated carbon for the adsorption of TGFs from *Ginkgo biloba* extract was higher than the Freundlich simulated adsorption coefficient, indicating that the adsorption of TGFs by activated carbon was more favorable to monolayer adsorption. Meanwhile, the optimal adsorption temperature was 30 °C. A low temperature is conducive to adsorption, but at too low a temperature, the viscosity of TGFs and other substances increases and is not conducive to adsorption.

**2.2. Desorption of TGFs from Activated Carbon.** The adsorption of TGFs in EGB by activated carbon mainly depends on the reversible adsorption of Van der Waals force between molecules and the irreversible adsorption of surface acidic oxides, both of which are superior to nonpolar compounds in adsorbing polar compounds. Methods of desorption of TGFs are mainly involved with temperature-rising desorption (boiling water), displacement desorption (phenol, ammonia, or  $\text{CaCl}_2$ ), and ultrasonic desorption. Boiling water has a great influence on the stability of TGFs, and the effect of ammonia water is remarkable compared with several detergents. Therefore, the study would optimize the related factors by a single factor.

**2.2.1. Single-Factor Optimization.** The effects of three resolving agents (phenol, ammonia, or  $\text{CaCl}_2$ ) on the resolution of TGFs in activated carbon were compared, among which ammonia had the most significant effect. Therefore, we compared the elution rates of different concentrations of ammonia on TGFs resolved by activated carbon, and the results are shown in Figure 2A. The ammonia concentration reached its maximum at 5% but decreased gradually after exceeding 5%. Owing to the wide polarity range of flavonoids, the maximum desorption rate (71.2%) of TGFs can be achieved in about 5% ammonia–ethanol–water solution.

The extraction of TGFs by activated carbon is mainly carried out by hot water extraction and organic solvent extraction, which include ethanol, methanol, and acetone.<sup>14</sup> Considering the yield of the extract, the cost of the extraction solvent, and the safety of the product, ethanol aqueous solution was used as the extracting agent in this study. When the volumetric concentration of ethanol was 70%, the desorption rate of TGFs by activated carbon reached the maximum (Figure 2B). However, the fluctuations between 60 and 80% were very small. Because of the wide polarity range of flavonoids, alcohol-soluble and water-soluble flavonoids can reach the maximum desorption rate in 70% ethanol solution. When the concentration of ethanol exceeded 70%, the desorption rate of flavonoids decreased slowly.

Temperature can affect the resolution of TGFs to a certain extent. The desorption rate of flavonoids increased rapidly with the increase of temperature from 25 to 35 °C (Figure 2C). When the temperature was higher than 35 °C, the temperature had little effect on the desorption rate of flavonoids. Moreover, when the temperature is higher, it will not only increase the energy but may also change the chemical properties of flavonoids. Therefore, the optimal elution temperature was selected as 35 °C.

In addition, it showed that the desorption rate of TGFs increased with the increase of liquid volume; it increased linearly when the liquid volume was between 50 and 100 mL but slowly when the liquid volume exceeded 100 mL (Figure 2D).

**2.2.2. Box–Behnken Response Surface Analysis Scheme.** Due to the fact that single-factor optimization method is

troublesome and time-consuming and the interaction effects are often overlooked, a more powerful technique by which multiple variables can be optimized in relatively few experiments is urgently needed. Response surface methodology (RSM), a powerful mathematical and statistical technique, has been effectively used in testing multiple process factors and their inner active effects.<sup>15</sup> Based on a single factor optimization, the Box–Behnken response surface data analysis method was employed to optimize the conditions. First, the effects of four factors (ethanol volume, ethanol concentration, temperature, and ammonia concentration) and three levels in the process of activated carbon desorption of TGFs were investigated. The results are shown in Table 1.

**2.2.3. Response Surface Variance Analysis.** Design Expert V8.0 software was used to analyze the variance of the data. ANOVA was used to test the adequacy of the quadratic model, the results of which are shown in Table 2.

**Table 2. Model ANOVA Analysis of Variance**

sources	sum of squares	degree of freedom	mean square	F value	P value
model	1657.86	14	118.42	104.97	<0.0001
A-ethanol volume	356.10	1	356.10	315.65	<0.0001
B-ethanol concentration	644.75	1	644.75	571.50	<0.0001
C-temperature	49.35	1	49.35	43.75	<0.0001
D-ammonia concentration	1.97	1	1.97	1.74	0.2078
AB	6.33	1	6.33	5.61	0.0328
AC	12.43	1	12.43	11.01	0.0051
AD	13.43	1	13.43	11.91	0.0039
BC	43.03	1	43.03	38.14	<0.0001
BD	70.81	1	70.81	62.77	<0.0001
CD	1.24	1	1.24	1.10	0.3118
A <sup>2</sup>	137.13	1	137.13	121.55	<0.0001
B <sup>2</sup>	395.47	1	395.47	350.54	<0.0001
C <sup>2</sup>	15.95	1	15.95	14.14	0.0021
D <sup>2</sup>	24.55	1	24.55	21.76	0.0004
residual	15.79	14	1.13		
lack of fit	13.87	9	1.54	4.01	0.0911
pure error	1.92	5	0.38		
cor total	1673.66	28			
R <sup>2</sup>	0.9911				
adj. R <sup>2</sup>	0.9825				

The response value of TGFs extracted from *Ginkgo biloba* was tested by four factors and three levels of response surface design. Using Design Expert V8.0 software, the variance of the data regression equation in Table 3 was analyzed.

Generally, the  $F$ -value and  $P$ -value reflect the importance of each coefficient in the model equation. For a specific coefficient, the  $P$ -values substantiate the significance of each of the model terms, which is used as a tool to verify the significance of the coefficients and is representative of the interaction power of each independent variable factor. In addition, the larger  $F$ -value designates the significant corresponding coefficient terms.  $P$ -values < 0.05 indicate that the corresponding factors have a significant impact on the response value. From the results of variance analysis, we can conclude that our model ANOVA calculated an  $F$ -value of 104.97, the  $P$ -value of the model was less than 0.05, and the missing item  $P > 0.1$ , which indicated that the

Table 3. Response Surface Experimental Design Scheme and Results

serial number	A ethanol volume/mL	B ethanol concentration/%	C temperature/°C	D ammonia concentration/%	desorption rate/%	
					measured values/%	predicted values/%
1	75	40	35	5	46.52	45.33
2	100	40	35	5	53.45	53.71
3	75	80	35	5	58.12	57.48
4	125	80	35	5	70.08	70.89
5	100	60	25	3	62.84	63.31
6	100	60	45	7	67.38	66.84
7	100	60	25	7	64.14	63.76
8	100	60	45	7	67.15	66.84
9	75	60	35	3	54.58	55.87
10	125	60	35	3	70.77	70.43
11	75	60	35	7	58.15	58.67
12	125	60	35	7	67.01	65.90
13	100	40	25	5	46.25	47.07
14	100	80	25	5	69.21	68.29
15	100	40	45	5	56.9	58.01
16	100	80	45	5	66.74	66.11
17	75	60	25	5	53.8	53.71
18	125	60	25	5	68.04	68.13
19	75	60	45	5	61.52	61.62
20	125	60	45	5	68.71	68.99
21	100	40	35	3	58.09	56.78
22	100	80	35	3	63.14	63.03
23	100	40	35	7	47.2	47.51
24	100	80	35	7	69.08	70.58
25	100	60	35	5	69.91	69.4
26	100	60	35	5	68.84	69.4
27	100	60	35	5	69.7	69.4
28	100	60	35	5	70.05	69.4
29	100	60	35	5	68.5	69.4

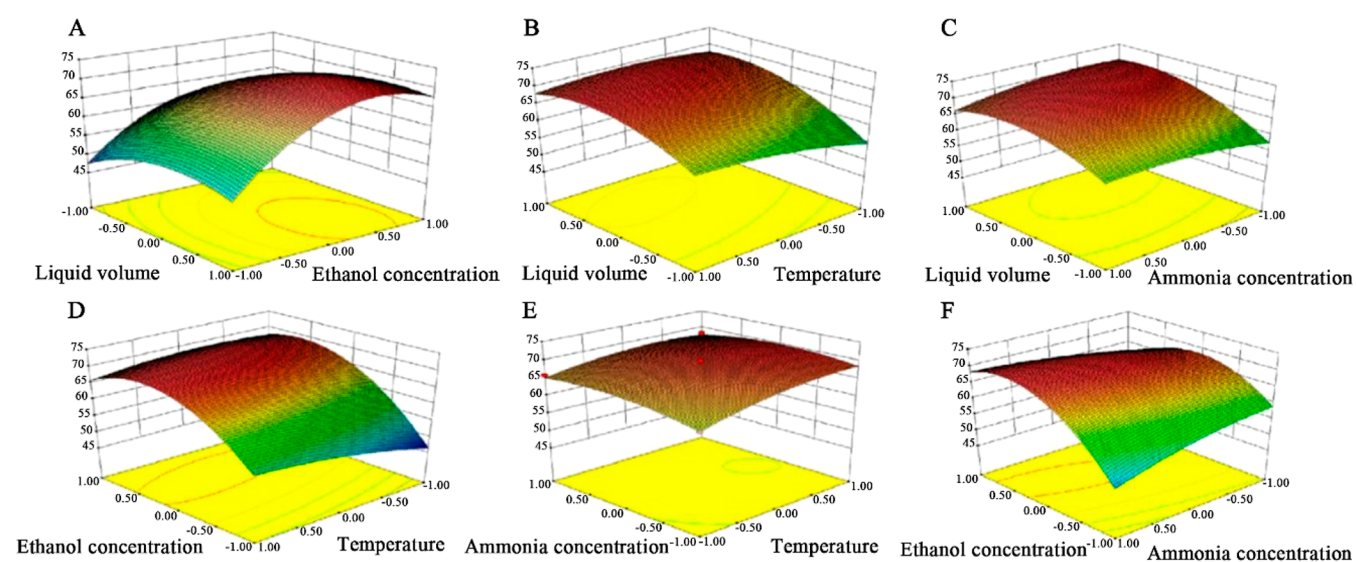


**Figure 3.** Response surface diagram of the effect of the interaction of two factors on the total flavone desorption rate. (A) Interaction of the elution ethanol volume and ethanol concentration. (B) Interaction of the elution ethanol volume and temperature. (C) Interaction of the ammonia concentration and elution ethanol volume. (D) Interaction of the ethanol concentration and temperature. (E) Interaction of the ammonia concentration and temperature. (F) Interaction of the ammonia concentration and ethanol concentration.

model was significant at the 1% level of significance, that is, the model fitted well in the whole regression region. The correlation coefficient  $R^2$  of the model was 0.9912, and the adjusted multiple correlation coefficient was 0.9825. Therefore, the selected

model was significant, the missing item was not significant, and the credibility of the model can be preliminarily judged to be high. The quadratic regression equation obtained can predict the corresponding response values well, and the fitting degree was

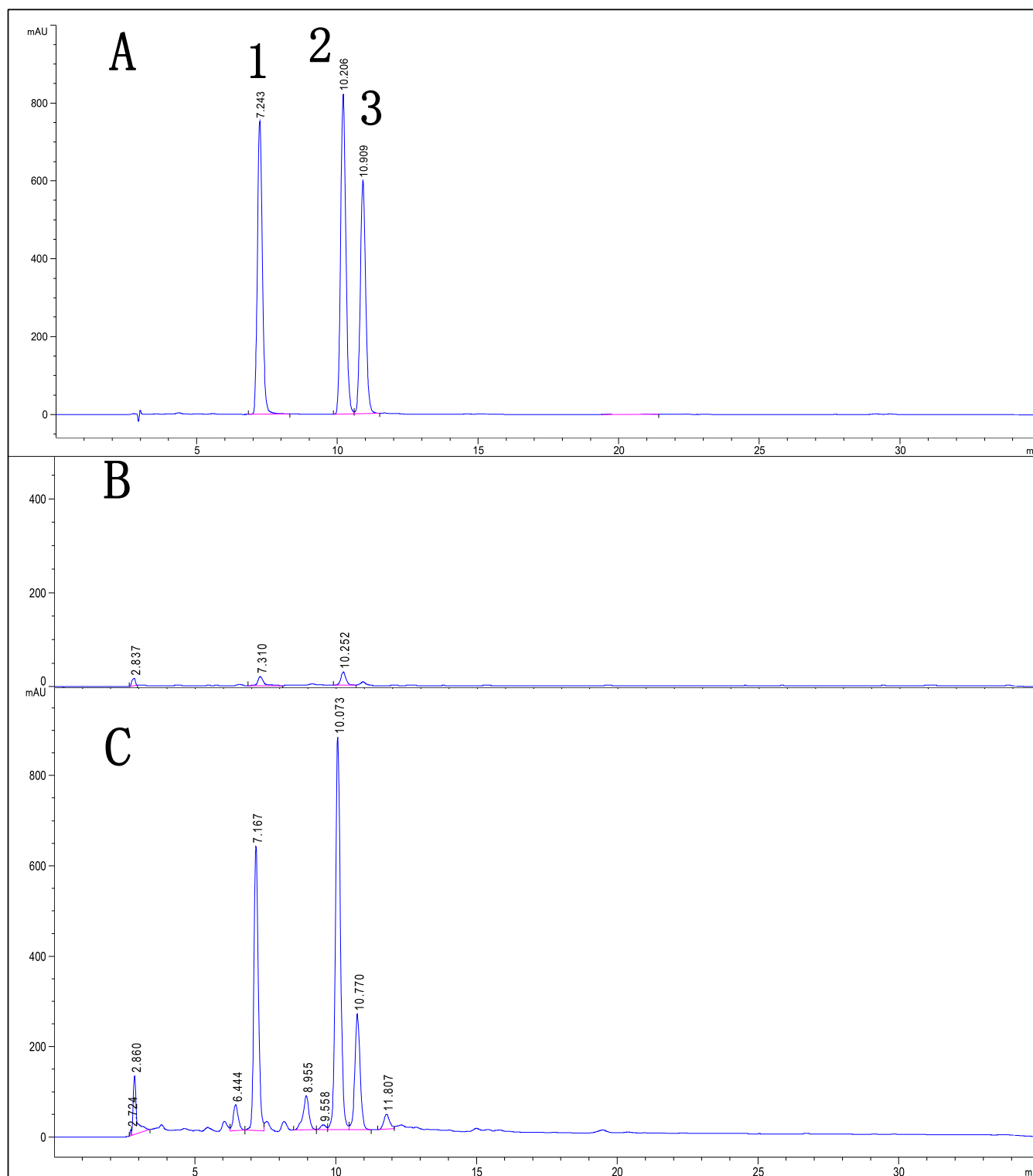


**Figure 4.** Hydrolysis of 70% ethanol and 70% ethanol + 5% ammonia eluent by HPLC after active carbon adsorption. (A) *Ginkgo* flavonoid aglycone mixed reference substance. (B) Hydrolysis of 70% ethanol. (C) Hydrolysis of 70% ethanol + 5% ammonia (1. quercetin; 2. kaempferol; 3. isorhamnetin).

proved to be good. Among the four factors studied by RSM, the ethanol volume, the ethanol concentration, and the temperature had significant effects, while ammonia concentration had no significant effects. RSM ANOVA analysis showed that  $F$  (ethanol concentration) >  $F$  (ethanol volume) >  $F$  (temperature) >  $F$  (ammonia concentration), which meant that the

order of influence of each factor on the yield of TGFs was ethanol concentration, liquid volume, temperature, and ammonia concentration.

Based on the changing trend of response surface and the degree of sparsity of the contour, it is seen that the interaction among the volumes of A (ethanol volume), B (ethanol

concentration), C (temperature), and D (ammonia concentration) has an effect on the desorption rate of TGFs in EGB. According to the regression equation of model prediction, the corresponding surface graph was obtained as shown in Figure 3. When the contour was circular, the interaction between the two factors was not obvious. On the contrary, when the contour was elliptical or saddle-shaped, the interaction between the two factors was obvious. The interaction effects of the response surface of each factor are as follows:

The ethanol concentration showed an obvious quadratic parabolic relationship with the desorption rate of TGFs, the response surface of the ethanol volume and ethanol concentration was elliptical with a steep slope of the response surface (Figure 3A), and the interaction between the ethanol volume and ethanol concentration was extremely significant. The desorption rate of TGFs increased with the increase of ethanol volume and ethanol concentration, and it was shown on the surface that the higher ethanol concentration and the larger ethanol volume were favorable to the increase of the desorption of TGFs. Based on the principle of similar solubility, the concentration of ethanol was in the range of 60–80% when the polarity of the eluent and the polarity of the main TGFs were the same, which promoted the desorption, and the desorption rate reached a peak.

The response surface of elution ethanol volume versus temperature was circular with a gentle slope of the response surface (Figure 3B), and the interaction between the two factors of elution ethanol volume and temperature was significant. Under the premise of constant temperature, the desorption rate of TGFs increased with the increase of elution ethanol volume; when the elution ethanol volume remained unchanged, the effect of increasing temperature on the desorption rate of TGFs was not obvious.

As to the interaction between the ammonia concentration and the elution ethanol volume, the response surface was round, the slope of the response surface was gentle, and the interaction between the ammonia concentration and the eluent volume was not obvious (Figure 3C). Under the premise of constant ammonia concentration, the TGF desorption rate increased with the increase of ethanol volume. Under the condition that the volume of eluted ethanol was small, the desorption rate of TGFs slightly decreased with the increase of ammonia concentration. Although the increase of ammonia concentration was beneficial to desorption, the decrease of the ethanol volume and the decrease of the dissolved TGF load were still not conducive to the increase of desorption rate.

As to the interaction between the ethanol concentration and temperature, the response surface was elliptical, the slope of the response surface was steep, and the interaction between the ethanol concentration and the temperature was significant (Figure 3D). Under the premise of constant ethanol concentration, the desorption rate of TGFs increased slowly with the increase of temperature, while under the premise of constant temperature, the desorption rate of TGFs increased significantly with the increase of ethanol concentration. At the concentration of 60–80% ethanol, the desorption rate of TGFs reached its peak.

The response surface of the interaction effect of ammonia concentration and the temperature was elliptical, the slope of the response surface was gentle, and the interaction effect of two factors, ammonia concentration and temperature, was not obvious (Figure 3E). Under the premise of constant ammonia concentration, the desorption rate of TGFs increased slowly

with the increase of temperature; under the premise of constant suitable temperature, the desorption rate of TGFs peaked with the change of ammonia concentration. Under the premise of constant temperature, the desorption rate peaked with the increase of ammonia concentration and then decreased, indicating that the increase of temperature would increase the volatilization of ammonia, and in addition, the increase of other substances dissolved in the eluent increased the viscosity leading to the decrease of the desorption rate of flavonoids.

The response surface of the interaction between the ethanol concentration and the ammonia concentration was elliptical, the slope of the response surface was steep, and the interaction between the two factors, ethanol concentration and ammonia concentration, was obvious (Figure 3F). Under the premise of very low ammonia concentration, a large ethanol concentration was needed to increase the TGF desorption rate; under the premise of constant ethanol concentration, the TGF desorption rate showed a great value with the change of ammonia concentration. When the concentration of ethanol is about 40%, the concentration of ammonia increases, but the desorption rate of flavonoids decreases because the low concentration of ethanol is not conducive to the dissolution of TGFs and decreases the desorption rate.

**2.2.4. Prediction and Verification of Optimum Desorption Conditions.** The data were further analyzed by Design Expert V8.0 software to determine the optimal conditions and regression model to analyze the best process conditions for the desorption of TGFs from activated carbon. The optimum technological conditions for the desorption of TGFs from activated carbon were as follows: eluent ethanol volume of 116.75 mL, ethanol concentration of 73.4%, elution temperature of 31.5 °C, and ammonia concentration of 5.7%. For the theoretical TGFs, desorption obtained under these conditions was 73.25%. According to the optimum conditions, three experiments were conducted to verify the adsorption of TGFs by all activated carbons, and the desorption rate was  $74.56 \pm 1.24\%$ .

**2.3. Chromatographic Analysis and Microscopic Morphology Analysis of TGFs Desorbed by Activated Carbon.** The TGFs in EGB were adsorbed by saturated static adsorption of activated carbon. After 4 h of adsorption, the TGFs were eluted by 70% ethanol and then desorbed down by adding 70% ethanol and 5% ammonia water. The prepared sample of TGFs was HPLC chromatographed after acid hydrolysis. After a 1 mL sample was hydrolyzed, the results are shown in Figure 4. As shown in Figure 4, 70% ethanol could not be eluted by activated carbon after adsorbing TGFs, while 70 and 5% ammonia water can elute and adsorb TGFs. Quercetin, kaempferol, and isorhamnetin are the main flavonoid glycosides of TGFs, which are similar to the flavonoid types of Ginkgo extracts.

To understand the changes of activated carbon before and after ammonia hydrolysis and adsorption, the activated carbon was dried at low temperatures before and after ammonia hydrolysis and adsorption, respectively. Meanwhile, its micro-morphology was displayed by SEM. The structure of the surface layer scanned by scanning electron microscopy (SEM) at a magnification of 1000 and 2000 is shown in Figure 5. Under the electron microscope, it can be seen that Figure 5A had a light yellowish material adsorbed on the surface, which was tentatively inferred to be the TGF adsorbate, while the obvious yellowish spots cannot be seen in Figure 5B. After elution, the particle size of B was larger; the radius of small ones was more than 5  $\mu\text{m}$ , and the length of large ones was close to 100  $\mu\text{m}$ . In

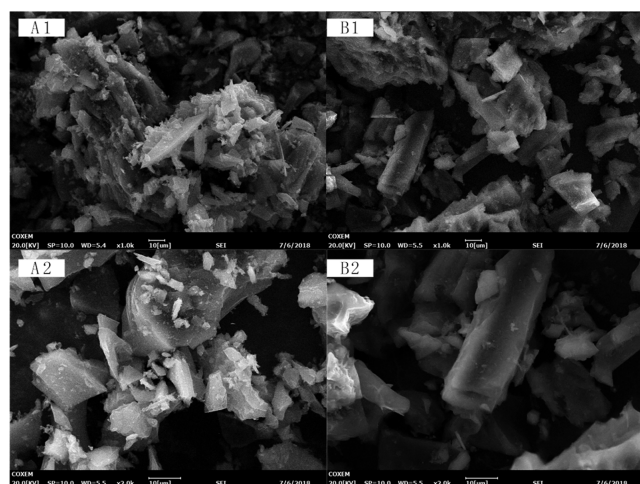


**Figure 5.** SEM of TGFs adsorbed by activated carbon and desorbed. A<sub>1</sub> and A<sub>2</sub> are SEM photos with different magnifications before elution. B<sub>1</sub> and B<sub>2</sub> are SEM photos with different magnifications after elution. (A<sub>1</sub> and A<sub>2</sub> magnify 1000 and 2000 times; B<sub>1</sub> and B<sub>2</sub> magnify 1000 and 2000 times; bar = 10  $\mu\text{m}$ ). The parameters set by SEM are acceleration voltage 20 kV, working distance 5 mm, and beam spot size 10 pA.

contrast, the small particles with a radius of less than 5  $\mu\text{m}$  were seen in A after 1000 and 2000 magnification. Activated carbons in Figure 5A,B were mostly stacked together, and the particle size distribution was uneven, ranging from 1 to 100  $\mu\text{m}$ . The adsorbed TGFs could not be eluted by different concentrations of ethanol from the activated carbon but could be cleaned by the mixture of ethanol and ammonia. The richer the acidic compounds in the oxygen-containing functional groups on the surface of activated carbon, the higher the efficiency of adsorption of polar compounds. The activated carbon is very easy to form dead adsorption with TGFs, and the addition of ammonia can destroy the role of acidic oxygen-containing groups of activated carbon after desorption of TGFs.

## 2.4. Static and Dynamic Desorption Curves of TGFs Adsorbed by Activated Carbon.

To further obtain the desorption behavior of activated carbon under the optimal desorption process conditions, the relationship between the desorption TGFs of activated carbon and time was investigated. The eluates of adsorption and desorption were collected at different time points. The kinetic curves of static adsorption and desorption of activated carbon on TGFs in EGB are shown in Figure 6A. According to the static desorption curve of TGFs adsorbed by activated carbon, the desorption amount of TGFs by activated carbon increased significantly with time. The whole process can be divided into three stages: the desorption index increased in 0–10 min, the linear growth period; the equilibrium state of desorption approached in 10–90 min, the slow growth period; the desorption amount stabilized to a fixed value after 90 min. To ensure complete desorption, the last experimental period lasted 4 h.

To understand the distribution of TGFs desorbed by activated carbon under the optimum desorption conditions, the TGFs were first absorbed to saturation and then eluted with distilled water of twice volume and 40% ethanol. Then, gradient elution was carried out by ethanol at different concentrations plus 5% ammonia water. The desorption solution was collected in different stages, and the concentrations of three flavonoid glycosides and total flavonoids in the effluent were determined. The results are displayed in Figure 6B. The highest concentration of TGFs could be obtained when 2BV was eluted by 40% ethanol + 5% ammonia water. After elution by 60% ethanol + 5% ammonia water 2BV, the concentration of flavonoids in *Ginkgo biloba* leaves decreased significantly, although it maintained a gentle level. The dynamic desorption curve showed that the active carbon completely adsorbed TGFs and dynamically desorbed 60% ethanol + 5% ammonia water to elute 4 times the column volume, and the TGFs in the column were desorbed. When 40% ethanol + 5% ammonia was hydrolyzed and absorbed, the maximum concentration of TGFs could reach 3.75 mg/mL. There was a force between

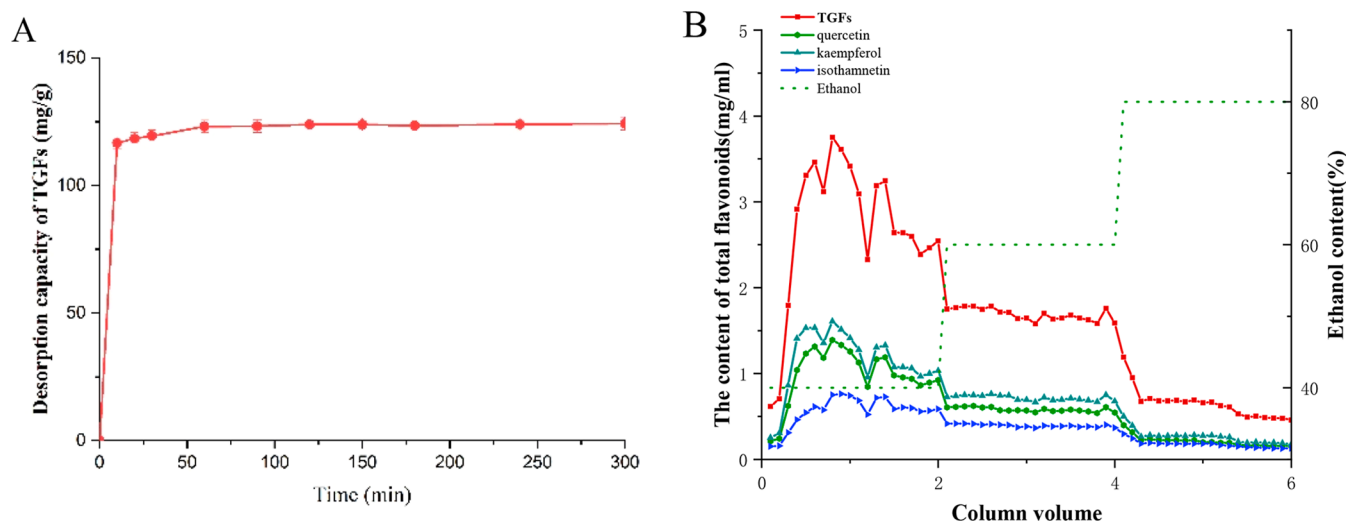


**Figure 6.** Desorption kinetics curve of activated carbon on TGFs (A) and dynamic desorption curve of TGFs adsorbed by activated carbon with different ethanol concentrations (B). (A) Activated carbon saturated by static adsorption was eluted twice with 20% ethanol and 80% ethanol and 5% ammonia water, and then the desorption amount of TGFs was determined at 10–360 min. (B) 30 g of activated carbon was loaded into the column and 20 g of EGB was dissolved. After 6 h of full adsorption, the elution agent was 10% ethanol, 40% ethanol, 40% ethanol with 5% ammonia water, 60% ethanol with 5% ammonia water, and 80% ethanol with 5% ammonia water. Sampling was 1 mL; all eluates were collected and condensed into solids for refrigeration. The content of TGFs in EGB was taken as the ordinate, and the elution volume as abscissa in the desorption dynamic curve.

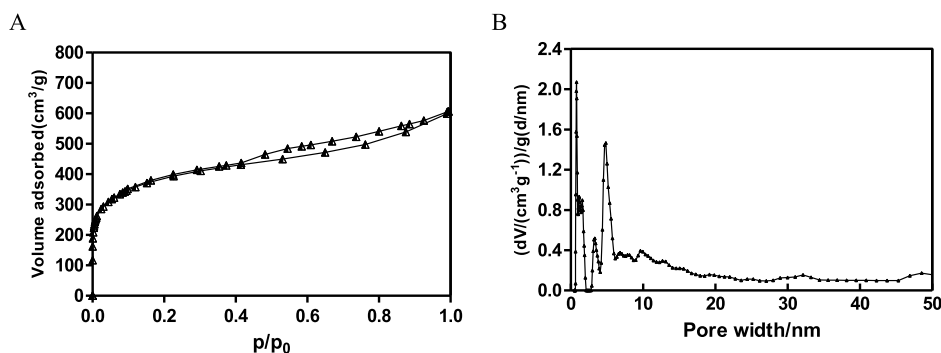


**Figure 7.** Nitrogen adsorption–desorption isotherms of the activated carbons (A) and pore size distributions of the activated carbon calculated by the QSDFT method (B). (A) Nitrogen adsorption isotherm of activated carbon was determined by the Autosorb-iQ2 adsorbent. (B) Pore size distribution was obtained by Quenched Solid Density Fund.

the flavonoids and the acidic oxygen-containing functional groups on the porous surface, so it is easy to form dead adsorption. A certain concentration of ammonia could damage the structure of the activated carbon surface, allowing the ginkgo flavonoids in the micropores and mesopores to be released more easily. At the same time, the addition of ammonia weakened the hydrogen bonding force between flavonoids and activated carbon, thus helping the *Ginkgo* flavonoids to be desorbed down.

**2.5. Analysis of Pore Structure and Pore Diameter Distribution of Activated Carbon.** The pore structure and pore size distribution of activated carbon were the main factors affecting the adsorption and desorption of flavone glycosides. The activated carbon used in this study was the preliminary optimized adsorption carrier for the relevant enterprises. Studying and understanding the pore structure and pore size distribution of the activated carbon was conducive to further improving the process of adsorbing and desorbing TGFs from *Ginkgo biloba* leaves and laying a foundation for the development of more suitable activated carbon.

The nitrogen adsorption–desorption isotherms of activated carbon were measured by the Autosorb-iQ2 adsorbent. The activated carbon used in this study had a well-developed pore structure with a specific surface area of more than  $1447.68 \text{ m}^2 \cdot \text{g}^{-1}$ . According to the International Union of Pure and Applied Chemistry (IUPAC) classification, the adsorption isotherms of this activated carbon belong to type I isotherms, and they are microporous-based activated carbons with relatively highest specific surface area, largest microporous volume ( $V_{\text{mic}} = 0.514 \text{ cm}^3 \cdot \text{g}^{-1}$ ), and smaller mesoporous volume ( $V_{\text{mes}} = 0.493 \text{ cm}^3 \cdot \text{g}^{-1}$ ). Among them, the proportion of pore volume was greater than 49.3% ( $V_{\text{mes}}/V_{\text{T}}$ ), and the hysteresis regression circles of their adsorption–desorption isotherms are obvious. The calculated pore structure parameters are shown in Figure 7.

The optimum molecular weight of activated carbon adsorption was between 500 and 3000, and the molecular weight of TGFs was basically between 500 and 1000 with a large proportion of micropores and mesopores. TGFs were more likely to enter the micropores to form dead adsorption (Figure 7A). The results are beneficial to further improve the process of adsorption and desorption of TGFs and also lay the foundation for the screening of more suitable activated carbon. The pore size distribution of activated carbon was one of the main factors affecting its adsorption performance. The pore size distribution curve of the activated carbon is shown in Figure 7B. From the pore size distribution curve of activated carbon, it was shown that the pore size distribution of activated carbon was relatively wide. The micropore size of activated carbon was mainly

concentrated in 0.64 and 1.00 nm, and the mesopore size was mainly concentrated in the range of 2.89–39.5 nm.

### 3. CONCLUSIONS

In this paper, the adsorption of TGFs by activated carbon was studied. The method of desorption of ginkgo flavonoids in this paper has not been reported in the literature. This method can well recycle the flavonoids adsorbed in waste activated carbon, but the experiment is still under research and has not been scaled up in the factory. The maximum adsorption capacity of activated carbon for TGFs was  $226.7 \text{ mg/g}$  activated carbon when pH was 5 and the temperature was  $30 \text{ }^\circ\text{C}$ . The adsorption coefficient fitted by Langmuir isotherm and Freundlich showed that the adsorption of TGFs by activated carbon was more effective and inclined to monolayer adsorption. After the activated carbon adsorbed the TGFs, it produced dead adsorption, and ethanol with different concentrations could not achieve desorption. Then, the process of activated carbon desorption of TGFs was optimized, which provided a feasible method for the recovery and utilization of TGFs. Optimum desorption conditions obtained by RSM were as follows: elution volume 116.75 mL, ethanol concentration 73.4%, elution temperature  $31.5 \text{ }^\circ\text{C}$ , and ammonia concentration 5.7%. The desorption rate of TGFs can reach to 74.56%. The pore structure and pore size distribution of activated carbon before and after TGF desorption were analyzed by SEM. Activated carbon has a wide pore size distribution. The micropore size is mainly about 0.64 and 1.0 nm, and the mesoporous size is mainly between 2.89 and 39.5 nm. The molecular weight of TGFs was mainly distributed between 500 and 1000 Da, which can be transported to the micropore through the mesoporous channel. On the other hand, there was a force between the flavonoids and the acidic oxygen-containing functional groups on the porous surface, so it is easy to form dead adsorption. Studying and understanding the pore structure and pore size distribution of the activated carbon will help to further improve the process of adsorption and desorption of TGFs from *Ginkgo biloba* leaves and lay a foundation for the development of more suitable activated carbon. Through the optimization of the process, it is expected that simultaneously preparing ginkgolide and effectively utilizing TGFs can be feasible.

### 4. EXPERIMENTAL SECTION

**4.1. Materials and Instruments.** EGB and activated carbon were provided by Jiangsu Kanion Pharmaceutical Co., Ltd. (Lianyungang, China). Quercetin (1), kaempferol (2), and

isorhamnetin (3) standards (98% purity) were purchased from Chengdu Must Biological Technology Co., Ltd. (Chengdu, China). Other chemical reagents were of analytical grade and obtained from Guoyao Chemical Reagent Co., Ltd. (Shanghai, China). The instruments used were a B-100 rotary evaporator (Switzerland Buchi), a ZHWY200D incubator shaker (Shanghai Zhicheng, China), a COXEM-30PLUS SEM (Kussem Company, Korea) microscope, Autosorb-iQ2 adsorbent (Quantachrome Company, USA), and glass chromatographic columns (Nanjing Wanqing Instruments, China).

**4.2. Determination of TGF Content.** Samples for TGFs analysis were prepared using the modified acid hydrolysis method described by Hasler and Sticher.<sup>11,16</sup> Accurately measured samples (500  $\mu\text{L}$ ) were transferred to 2 mL tubes; then, 500  $\mu\text{L}$  of methanol/25% HCl (4:1,  $v/v$ ) solution was added, and the mixture was refluxed at 75  $^{\circ}\text{C}$  for 2 h. The hydrolysis solutions were appropriately diluted with methanol and then filtered through membrane filters (0.22  $\mu\text{m}$ ). The content could be calculated according to the previous ref 17, shown as eq 1

$$\begin{aligned} &\text{TGFs content (mg/mL)} \\ &= (\text{quercetin content} + \text{kaempferol content} \\ &\quad + \text{isorhamnetin content}) \times 2.51 \end{aligned} \quad (1)$$

The components of TGFs were analyzed using a HPLC 1200 system (DAD; Agilent, USA) and a reverse phase C18 column (4.6  $\times$  250 mm, 5  $\mu\text{m}$ ; Agilent, USA) with a solvent system of water (A)-methanol (B). Gradient elution: 50% B run 0–12 min, 50% B–80% B 13–15 min, and 50% B 15–16 min. The flow ratio was 0.8 mL/min, the column temperature was 38  $^{\circ}\text{C}$ , and the detection wavelength was 360 nm.<sup>18</sup> Contents of hydrolytic aglycones quercetin (Q), kaempferol (K), and isorhamnetin (I) were 8.93, 9.88, and 6.11%, respectively.

**4.3. Determination of Static Adsorption and Desorption Curve of Activated Carbon.** Kinetic curve determination of adsorption and desorption of activated carbon: 1.5 g of activated carbon was accurately weighed and placed in a 250 mL triangular bottle with plug and grinding mouth; 1.5 g of EGB was added precisely; then, 100 mL of 10% ethanol was dissolved and sealed in a constant-temperature oscillator and oscillated at 30  $^{\circ}\text{C}$  for 180 rpm at 10, 20, 30, 60, 90, 120, 150, 180, 240, and 300 min. Sampling was 1 mL; the adsorption capacity and column loading of TGFs were determined.<sup>19,20</sup>

Activated carbon saturated by static adsorption was eluted twice with 200 mL of 20% ethanol and 200 mL of eluent with 80% ethanol and 5% ammonia water. The desorption amount of TGFs was determined at 10, 20, 30, 60, 90, 120, 150, 180, 240, 300, and 360 min.<sup>21,22</sup>

**4.4. Effect of pH Value on Adsorption of TGFs by Activated Carbon.** The pH value of the sample solution of EGB was adjusted to 3, 5, 7, and 9. Activated carbon (0.2 g) was precisely weighed, and EGB was dissolved in 100 mL of 10% ethanol. Adsorption equilibrium of TGFs on activated carbon was determined after 180 r/min oscillation for 6 h at 30  $^{\circ}\text{C}$  in a constant-temperature oscillator.

**4.5. Isotherm of TGFs Adsorbed by Activated Carbon.** Three groups of 5 parts of activated carbon with a mass of 0.2, 0.3, 0.4, 0.5, and 0.6 were added. Each group was oscillated at 25, 30, and 35 degrees centigrade in 180 r/min thermostat oscillators for 6 h. After reaching the adsorption equilibrium, the concentration of TGFs was determined. The equilibrium

adsorption capacity was ordinate and the equilibrium concentration was abscissa. The adsorption isotherms under different conditions were obtained. The experimental results were fitted by the Langmuir equation (eq 2) and the Freundlich equation<sup>23</sup> (eq 3).

Langmuir isotherms

$$Q_e = \frac{Q_m \times K_L \times C_e}{1 + K_L \times C_e} \quad (2)$$

Freundlich isotherms

$$Q_e = K_F \times C_e^{1/n} \quad (3)$$

$K_L$  (mg/mL) is the Langmuir constant,  $Q_m$  and  $1/n$  are empirical constants, and  $K_F$  is the Freundlich constant that is an indicator of adsorption capacity.  $Q_e$  is the maximum adsorption capacity (mg/g), and  $C_e$  is the concentration at equilibrium (mg/mL).

**4.6. Dynamic Desorption Curve of TGFs Adsorbed by Activated Carbon.** Activated carbon (30 g) was loaded into the column (about 10 cm in height, 3 cm in diameter, and 70 mL in volume). EGB (20 g) was dissolved, the solution of which was prepared into 50 mg/mL 400 mL using 10% ethanol. After 6 h of full adsorption, the elution agent (140 mL) was 10% ethanol and 40% ethanol in order, then 40% ethanol with 5% ammonia water, 60% ethanol with 5% ammonia water, and 80% ethanol with 5% ammonia water. The flow rate was controlled at 2BV/h. Sampling was 1 mL at 7 mL intervals, and all eluents were collected and condensed into solids for refrigeration. The content of TGFs in EGB was taken as the ordinate and the elution volume as abscissa in the desorption dynamic curve.<sup>24,25</sup>

**4.7. Desorption Technology of TGFs from Activated Carbon.** **4.7.1. Single-Factor Experiment.** In each group, 0.75 g of EGB was dissolved in 50 mL of 20% ethanol solution and adsorbed by 1.5 g of activated carbon for elution experiment. Single-factor experiments were carried out with water as the solvent, the volume of ammonia-ethanol-distilled water solution, the concentration of ammonia-water, the concentration of ethanol, and extraction temperature.

The experimental scheme is described as follows:

The effects of solution volume on the extraction rate were 50, 75, 100, 125, and 150 mL. The effects of ammonia concentration on the extraction rate were 1, 3, 5, 7, and 9%. The effects of ethanol concentration on the extraction rate were 40, 50, 60, 70, and 80%. The effects of extraction temperature on the extraction rate were as follows: 25, 30, 35, 40, 45, 50, and 55  $^{\circ}\text{C}$ .

**4.7.2. RSM for Optimizing Activated Carbon Desorption of TGFs.** In each group, 0.75 g of EGB was dissolved in 50 mL of 20% ethanol solution and adsorbed by 1.5 g of activated carbon for the elution experiment. According to the single-factor experimental results and the Box-Behnken design principle, the liquid volume, the ammonia concentration, the ethanol concentration, the extraction temperature, and other four factors were selected for studying the elution process. The response value of TGFs extracted from *Ginkgo biloba* was tested by four factors and three levels of response surface design,<sup>26–28</sup> as shown in Table 3.

**4.8. Pore Structure Analysis of Activated Carbon.** The nitrogen adsorption isotherm of activated carbon was determined by an adsorbent of Autosorb-iQ2 (Quantachrome Company, USA). Before the test, the activated carbon sample was degassed at 250  $^{\circ}\text{C}$  for 12 h. Based on the nitrogen adsorption isotherm, the specific surface area ( $S_{\text{BET}}$ ) of activated carbon was calculated by the Brunauer Emmet Teller (BET)

equation,<sup>29</sup> while the total pore volume ( $V_{\text{tot}}$ ) was calculated by nitrogen adsorption at a relative pressure of 0.99 Mpa, and the micropore volume ( $V_{\text{mic}}$ ) was calculated by the Dubinin–Radushkevich equation.<sup>30</sup> The mesoporous volume ( $V_{\text{mes}}$ ) was obtained by subtracting the micropore volume from the total pore volume, and the pore size distribution was obtained by Quenched Solid Density Fund. The quenched solid density functional theory (QSDFT) equation could be used to calculate the specific surface area in a certain aperture range.<sup>31</sup>

**4.9. Microstructural Analysis.** The parameters set by SEM were acceleration voltage 20 kV, working distance 5 mm, and beam spot size 10 pA. The microanalysis of *Ginkgo* flavonoids adsorbed by activated carbon before and after elution was carried out by SEM at 1000 and 2000 times. Before observation, the microstructure of activated carbon samples can be observed directly.

## AUTHOR INFORMATION

### Corresponding Authors

**Wei Xiao** – Jiangsu Kanion Pharmaceutical Co., Ltd., Lianyungang, Jiangsu 222047, China; Phone: +86-0518-81152227; Email: [xw@kanion.com](mailto:xw@kanion.com)

**Linguo Zhao** – College of Chemical Engineering and Co-Innovation Center for Sustainable Forestry in Southern China, Nanjing Forestry University, Nanjing 210037, China; [orcid.org/0000-0002-8085-9557](https://orcid.org/0000-0002-8085-9557); Phone: +86-025-85427962; Email: [njfu2304@163.com](mailto:njfu2304@163.com)

### Authors

**Lihu Zhang** – College of Chemical Engineering, Nanjing Forestry University, Nanjing 210037, China; Department of Pharmacy, Jiangsu Vocational College of Medicine, Yancheng 224005, China

**Xiaomeng Zhang** – College of Chemical Engineering, Nanjing Forestry University, Nanjing 210037, China

**Qi Li** – College of Chemical Engineering and Co-Innovation Center for Sustainable Forestry in Southern China, Nanjing Forestry University, Nanjing 210037, China; [orcid.org/0000-0001-9181-1391](https://orcid.org/0000-0001-9181-1391)

**Erzheng Su** – Co-Innovation Center for Sustainable Forestry in Southern China, Nanjing Forestry University, Nanjing 210037, China; [orcid.org/0000-0002-3868-567X](https://orcid.org/0000-0002-3868-567X)

**Fuliang Cao** – Co-Innovation Center for Sustainable Forestry in Southern China, Nanjing Forestry University, Nanjing 210037, China

Complete contact information is available at:

<https://pubs.acs.org/10.1021/acsomega.1c05670>

### Author Contributions

Lihu Zhang and X.Z. contributed equally. Author contributions are as follows: Lihu Zhang, Linguo Zhao, F.C., and W.X. conceived and designed the experiments; Lihu Zhang and X.Z. performed all experiments and analyzed the data; Q.L. and E.S. helped to revise the paper. All authors have read and approved the manuscript.

### Notes

The authors declare no competing financial interest.

## ACKNOWLEDGMENTS

This work was supported by the Forestry Achievements of Science and Technology to Promote Projects ([2017] 10), the Jiangsu Provincial Policy Guidance Program (Grant no. SZ-

XZ2017023), the Yancheng Health College Institute of Biomedical Technology (Jiangsu province postdoctoral innovation practice base), and the Qing Lan Project of Jiangsu Province (2017).

## REFERENCES

- (1) Yoshikawa, T.; Naito, Y.; Kondo, M. *Ginkgo biloba* leaf extract: review of biological actions and clinical applications. *Antioxid. Redox Signaling* **1999**, *1*, 469–480.
- (2) Singh, B.; Kaur, P.; Gopichand; Singh, R. D.; Ahuja, P. S. Biology and chemistry of *Ginkgo biloba*. *Fitoterapia* **2008**, *79*, 401–418.
- (3) Van Beek, T. A.; Montoro, P. Chemical analysis and quality control of *Ginkgo biloba* leaves, extracts, and phytopharmaceuticals. *J. Chromatogr. A* **2009**, *1216*, 2002–2032.
- (4) Stromgaard, K.; Saito, D. R.; Shindou, H.; Ishii, S.; Shimizu, T.; Nakanishi, K. Ginkgolide derivatives for photolabeling studies: preparation and pharmacological evaluation. *J. Med. Chem.* **2002**, *45*, 4038–4046.
- (5) Nabavi, S. M.; Habtemariam, S.; Daglia, M.; Braidly, N.; Loizzo, M. R.; Tundis, R.; Nabavi, S. F. Neuroprotective effects of ginkgolide B against ischemic stroke: a review of current literature. *Curr. Top. Med. Chem.* **2015**, *15*, 2222.
- (6) Guo, X. F. Research advances in extraction, isolation, purification and content determination of methods flavonoids. *J. Anhui Agric. Sci.* **2007**, *35*, 8083–8086.
- (7) Goh, L. M.; Barlow, P. J.; Yong, C. S. Examination of antioxidant activity of *Ginkgo biloba* leaf infusions. *Food Chem.* **2003**, *82*, 275–282.
- (8) Lu, C.; Panb, L.; Zhuc, B. In study the static adsorption/desorption of formaldehyde on activated carbons. *2015 International Forum on Energy; Environment Science and Materials*, 2015.
- (9) Bedir, E.; Tatli, I. I.; Khan, R. A.; Zhao, J.; Takamatsu, S.; Walker, L. A.; Goldman, P.; Khan, I. A. Biologically active secondary metabolites from *Ginkgo biloba*. *J. Agric. Food Chem.* **2002**, *50*, 3150–3155.
- (10) van Beek, T. A.; Montoro, P. Chemical analysis and quality control of *Ginkgo biloba* leaves, extracts, and phytopharmaceuticals. *J. Chromatogr. A* **2009**, *1216*, 2002–2032.
- (11) Hasler, A.; Gross, G.-A.; Meier, B.; Sticher, O. Complex flavonol glycosides from the leaves of *Ginkgo biloba*. *Phytochemistry* **1992**, *31*, 1391–1394.
- (12) Cheng, M.; Meng, L. J.; Zhou, X. D.; Zou, H. L.; Zhou, G. X. Chemical constituents of flavonoids and their glycosides in *Melastoma dodecandrum*. *China J. Chin. Mater. Med.* **2014**, *39*, 3301–3305.
- (13) Patiha; Firdaus, M.; Wahyuningsih, S.; Nugrahaningtyas, K. D.; Hidayat, Y. Derivation and constants determination of the Freundlich and (fractal) Langmuir adsorption isotherms from kinetics. *IOP Conf. Ser. Mater. Sci. Eng.* **2018**, *333*, 012010.
- (14) Hu, L. J. Purification processes development of flavone and terpene from *Ginkgo* leaves. *Shaanxi Forest Sci. Technol.* **2012**, *5*, 34–36.
- (15) Maba, B.; Res, A.; Epo, A.; Lsv, A.; Lae, A. Response surface methodology (RSM) as a tool for optimization in analytical chemistry. *Talanta* **2008**, *76*, 965–977.
- (16) Hasler, A.; Sticher, O.; Meier, B. Identification and determination of the flavonoids from *Ginkgo biloba* by high-performance liquid chromatography. *J. Chromatogr. A* **1992**, *605*, 41–48.
- (17) Commission, C. P. *Pharmacopoeia of the People's Republic of China*; Chemical Industry Press: Beijing, 2015; pp 316–317.
- (18) Zhang, L.; Wu, T.; Xiao, W.; Wang, Z.; Ding, G.; Zhao, L. Enrichment and purification of total *Ginkgo* flavonoid O-glycosides from *Ginkgo biloba* extract with macroporous resin and evaluation of anti-inflammation activities *in vitro*. *Molecules* **2018**, *23*, 1167.
- (19) Chi, G.; Zhao, S.; Yagiz, Y.; Gu, L. Static, kinetic, and isotherm adsorption performances of macroporous adsorbent resins for recovery and enrichment of bioactive procyanidins from *Cranberry Pomace*. *J. Food Sci.* **2017**, *83*, 1249.
- (20) Bing, W.; Lehmann, J.; Hanley, K.; Hestrin, R.; Enders, A. Adsorption and desorption of ammonium by maple wood biochar as a function of oxidation and pH. *Chemosphere* **2015**, *138*, 120–126.

(21) Šnauko, M.; Berek, D. Liquid chromatography under limiting conditions of adsorption and limiting conditions of desorption for separation of complex polymers. The role of “flower-like” interactions of macromolecules. *Chromatographia* **2003**, *57*, S55–S59.

(22) Farrell, J. Tridendate arsenate complexation with ferric hydroxide and its effect on the kinetics of arsenate adsorption and desorption. *Chemosphere* **2017**, *184*, 1209–1214.

(23) Gessner, P. K.; Hasan, M. M. Freundlich and langmuir isotherms as models for the adsorption of toxicants on activated charcoal. *J. Pharm. Sci.* **2006**, *76*, 319–327.

(24) Mosavi, S. H.; Zare-Dorabei, R.; Beryhi, M. Rapid and effective ultrasonic-assisted adsorptive removal of congo red onto MOF-5 modified by CuCl<sub>2</sub> in ambient conditions: adsorption isotherms and kinetics studies. *ChemistrySelect* **2021**, *6*, 4432–4439.

(25) Mosavi, S. H.; Zare-Dorabei, R.; Beryhi, M. Microwave-assisted synthesis of metal-organic framework MIL-47 for effective adsorptive removal of dibenzothiophene from model fuel. *J. Iran. Chem. Soc.* **2020**, *18*, 709.

(26) Yao, Q.; Shen, Y.; Bu, L.; Yang, P.; Xu, Z.; Guo, X. Ultrasound-assisted aqueous extraction of total flavonoids and hydroxytyrosol from olive leaves optimized by response surface methodology. *Prep. Biochem. Biotechnol.* **2019**, *49*, 837–845.

(27) Jiao, M.; Wu, Z. L.; Liu, Y.; Liu, W.; Li, R. Surfactant-assisted separation of ginkgo flavonoids from *Ginkgo biloba* leaves using leaching and foam fractionation. *Asia-Pac. J. Chem. Eng.* **2016**, *11*, 664–672.

(28) Agarwal, C.; Máthé, K.; Hofmann, T.; Csóka, L. Ultrasound-assisted extraction of cannabinoids from *Cannabis sativa L.* optimized by response surface methodology. *J. Food Sci.* **2018**, *83*, 700.

(29) Qin, C.; Chen, Y.; Gao, J.-m. Manufacture and characterization of activated carbon from marigold straw (*Tagetes erecta L.*) by H<sub>3</sub>PO<sub>4</sub> chemical activation. *Mater. Lett.* **2014**, *135*, 123–126.

(30) Wu, J.; Strömqvist, M. E.; Claesson, O.; Fängmark, I. E.; Hammarström, L.-G. A systematic approach for modelling the affinity coefficient in the Dubinin-Radushkevich equation. *Carbon* **2002**, *40*, 2587–2596.

(31) Kowalczyk, P.; Terzyk, A. P.; Gauden, P. A.; Leboda, R.; Szmeczig-Gauden, E.; Rychlicki, G.; Ryu, Z.; Rong, H. Estimation of the pore-size distribution function from the nitrogen adsorption isotherm. Comparison of density functional theory and the method of Do and co-workers. *Carbon* **2003**, *41*, 1113–1125.